



Engineering Demand Parameters for Acceleration-Sensitive Nonstructural Components: Comparison between Peak Floor Acceleration and Spectral Acceleration

Amir Banihashemi¹, Lydell Wiebe^{2*}, André Filiatrault³

¹ Ph.D. Candidate, Department of Civil Engineering, McMaster University, Hamilton, ON, Canada

² Professor, Department of Civil Engineering, McMaster University, Hamilton, ON, Canada

³ Professor, Department of Civil Engineering, University School for Advanced Studies IUSS Pavia, Pavia, Italy

* wiebel@mcmaster.ca (Corresponding Author)

ABSTRACT

The current FEMA P58 library provides damage fragility curves of acceleration-sensitive nonstructural components based on peak floor accelerations (PFAs). A shortcoming of PFA as an engineering demand parameter (EDP) is that it is independent of the period of components. As an alternative EDP for damage fragility curves, this study considers the spectral accelerations (Sa) at the period of the nonstructural component. To achieve this, nonstructural components with a range of periods between 0.01 and 1 second were designed for different strength levels and modeled in OpenSees using single-degree-of-freedom (SDOF) components with an elastic perfectly plastic material. The nonlinear time-history analyses for the SDOFs were performed using floor motions from the first and top floors of a six-story steel buckling-restrained braced frame. The effectiveness of PFA and Sa as EDPs was assessed by considering two efficiency and relative sufficiency criteria. The results show that although using Sa as the EDP is more efficient than using PFA for nonstructural components mounted on the lower floors, both the PFA and the Sa have similar efficiency for nonstructural components on the upper floors due to floor motion frequency content filtering caused by the structure's natural frequencies. Also, for almost all considered period ranges and strength levels of nonstructural components, using Sa is more sufficient than using PFA.

Keywords: Damage fragility curves, Nonstructural components, Engineering demand parameters (EDPs), Single-degree-of-freedom (SDOF) components, Numerical analysis.

INTRODUCTION

Studying the aftermath of recent earthquakes shows the considerable contribution of nonstructural components to economic losses [1,2]. Nonstructural components are generally divided into two categories: displacement-sensitive and acceleration-sensitive. Damage to displacement-sensitive nonstructural components is assessed directly through the inter-story drift of buildings. Conversely, for acceleration-sensitive nonstructural components, since inertia forces can cause overturning or excessive displacements of the components, their damage is indirectly evaluated using a parameter that is linked to floor accelerations. The current FEMA P58 [3] library uses peak floor accelerations (PFAs) for damage fragility curves of such nonstructural components. However, the efficiency of PFA to correlate with damage is limited because it does not consider the period of the component.

There is already a well-established set of engineering demand parameters (EDPs) that represent the response of a structure to an earthquake, as described through ground motion intensity measures (IMs). Examples of EDPs include the maximum displacement at the roof, the PFA, and the floor response spectrum. Examples of IMs include the PGA and the ground response spectrum. Historically, PGAs were once used as the primary IM of ground motions. However, with the advancement of response spectra theory [4,5], the spectral acceleration at the fundamental period of a structure became the prevalent IM in earthquake engineering. Although several studies in the last decade have proposed alternate IMs, this parameter is still the most used IM in procedures for assessing the seismic performance of buildings. Also, as IMs and EDPs are random variables showing high dispersion [6], many statistical approaches have been developed [7–9] to extract information from EDP-IM pairs to select the most suitable IM.

Just as previous studies have sought ground motion IMs that would predict the structural response in terms of EDPs, there is a need to understand structural EDPs that will predict the non-structural damage. However, unlike the many studies on selecting of a suitable IM for the prediction of EDPs in buildings, to the best knowledge of the authors, there are no studies comparing the performance of EDPs in assessing damage for acceleration-sensitive nonstructural components. Not only can acceleration-sensitive nonstructural components be the source of significant seismic losses, but the characteristics of the floor motions they experience during earthquakes may also differ as they are installed on various floors of buildings, which may filter the ground motion frequency content. To shed some light on this issue, this study aims to compare PFA and the spectral acceleration at the period of acceleration-sensitive nonstructural component (S_a) to identify the more suitable EDP for damage fragility curves of nonstructural components. For this purpose, nonstructural components, modeled as elastic perfectly plastic single-degree-of-freedom (SDOF) components, are subjected to floor motions resulting from nonlinear time-history analyses of a code-compliant six-story steel buckling-restrained braced frame. Then, statistical efficiency and sufficiency studies are used to identify the more suitable EDP by comparing ductility-PFA and ductility- S_a pairs resulting from the numerical analyses.

FLOOR MOTION DATABASE AND MODELING OF ACCELERATION-SENSITIVE NONSTRUCTURAL COMPONENTS

In this study, a six-story office building with a plan area of 2010 m² and a story height of 4.57 m was designed using buckling-restrained braced frames. The building is assumed to be located in a high seismicity area in the United States with a seismic category D and mapped short-period and 1-second spectral accelerations of $S_s=1.5$ g and $S_1=0.5$ g [10], respectively. The numerical model of the building was developed using the OpenSees platform [11] based on analytical modeling and calibrated data for the behavior of buckling resistance braces suggested by Zsarnóczy [12]. The nonlinear time-history analyses were performed using the suite of 44 far-field ground motion records recommended by FEMA P695 [13]. The selected suite was scaled at six intensity levels: 0.25, 0.50, and 1.0 times the design earthquake (DE), and 1.0, 1.5, and 2.0 of the maximum considered earthquake (MCE). Figure 1 shows the individual records' and median acceleration floor response spectra for the first and roof levels of the building at the design earthquake (DE) level.

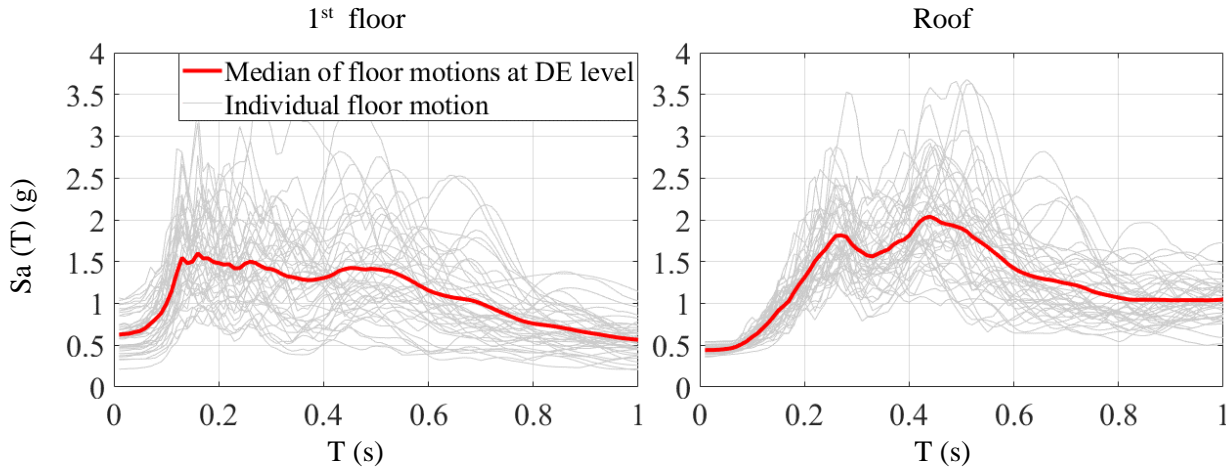


Figure 1: Median acceleration floor response spectra at the design earthquake (DE) level.

This study assumes that nonstructural components behave as damped SDOF nonstructural components and are rigidly attached to their supporting buildings. The SDOF nonstructural components' initial (elastic) periods ranged from 0.01 to 1 second, with increments of 0.01 s. The behavior of SDOF nonstructural components was modeled using a bilinear elastic-perfectly-plastic hysteresis model with no strain hardening and a damping ratio of 5%. The yield strength (f_y) of the hysteresis model was determined using the design earthquake (DE) level median acceleration floor response spectrum at the period of the SDOF nonstructural component as illustrated in Figure 1 divided by a response modification coefficient (R). To account for various levels of strength, three R values of 1.5, 2.0, and 3.0 were selected.

Nonlinear time-history analyses were performed on each SDOF nonstructural component subjected to the absolute floor acceleration time-history responses that were computed for the six intensity levels obtained from the nonlinear time-history analyses of the building. The ductility (μ) demands for the SDOF nonstructural components were estimated using either PFAs or S_a as seismic EDPs. As an example, Figure 2 shows the ductility demands in terms of PFA and S_a that were obtained for the SDOF nonstructural component with a nonstructural period of 0.6 s and R of 3, mounted on the first floor. For this component, the ductility reaches up to 20 at scaled floor motions of 1.5 to 2.0 MCE levels. At lower intensity levels, such as 0.25 and 0.5 DE, the component mostly has linear response with ductility less than 1. For this range of ductility, the results confirm a linear relationship between S_a and ductility.

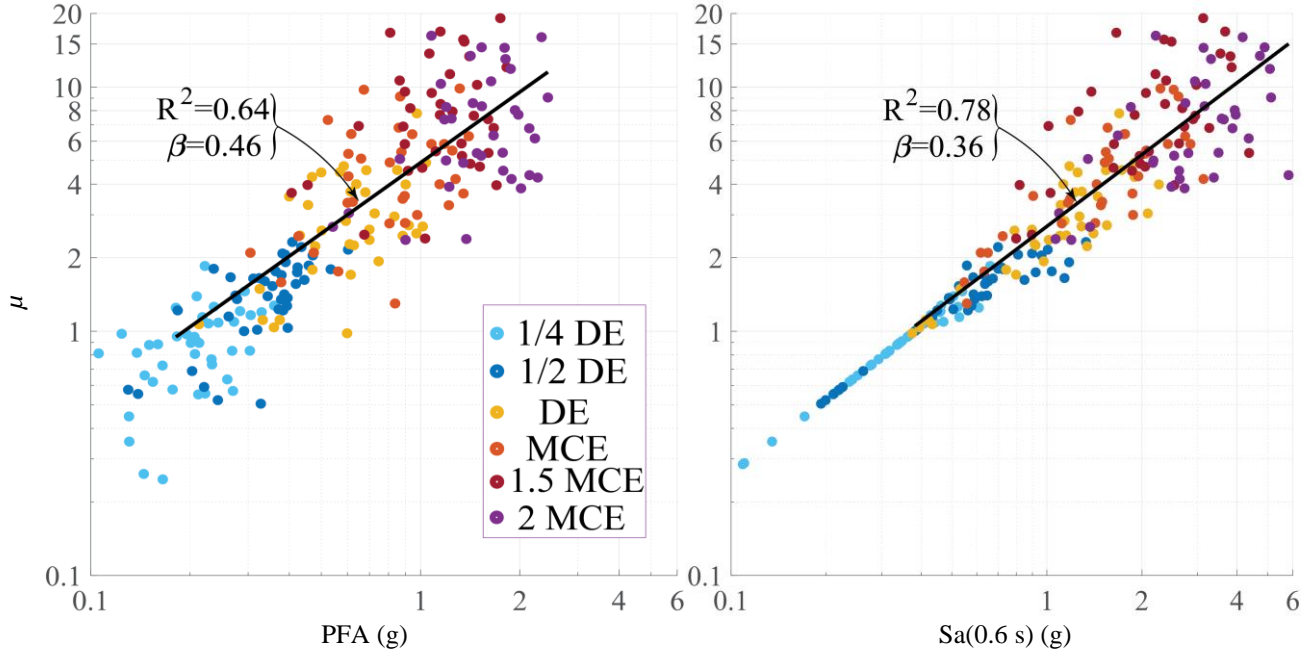


Figure 2: Ductility demands of the SDOF nonstructural component with a period of 0.6 s and R of 3, installed on the first floor, in terms of PFA and $S_a(0.6 \text{ s})$.

SEISMIC FRAGILITY EVALUATION

A fragility curve provides the probability of the seismic demand, in this study μ of the SDOF nonstructural components, surpassing a particular capacity level or damage state. A fragility curve is conditioned on an EDP. A fragility curve can be estimated using the standard normal cumulative distribution function using the below equation [14]:

$$P(\mu \geq C | EDP) = \Phi \left(\frac{\ln(M_d) - \ln(M_c)}{\sqrt{\beta_{d|EDP}^2 + \beta_c^2}} \right) \quad (1)$$

where M_d is the median of the μ estimate as a function of EDP, M_c is the median estimate of the capacity, $\beta_{d|EDP}$ is the logarithmic standard deviation of the demand conditioned on the EDP, β_c is the logarithmic standard deviation of the capacity, and Φ is the standard normal cumulative distribution.

The linear least squares method is employed herein to determine the median of the μ and the logarithmic standard deviation of μ given EDP. Using the power law model [7] and assuming that the standard deviation is constant with respect to the EDP [15], M_d and $\beta_{d|EDP}$ can be determined as follows:

$$M_d = aEDP^b \quad (2)$$

$$\beta_{d|EDP} = \sqrt{\frac{\sum_{i=1}^N [\ln(\mu_i) - \ln(aedp_i^b)]^2}{N - 2}} \quad (3)$$

In Eq. (2), a and b are the parameters of the regression. In Eq.(3), and for this study, N is the total number of floor acceleration time-history responses, and μ_i and edp_i denote the μ and EDP values, respectively, that are associated with the i^{th} floor acceleration time-history response. A linear regression model was developed for each SDOF nonstructural component using logarithmically transformed variables of the considered μ and EDPs. To ensure that the regression focuses on data that may be associated with component damage, only data with ductility demands greater than unity was included in the regression model. The regression model developed for the example in Figure 2 is shown with a solid black line for the μ -PFA and μ - S_a pairs, respectively.

EDP SELECTION CRITERIA

Whereas an ideal EDP would directly indicate the probability of damage, selecting a real acceleration-related EDP can greatly impact the uncertainty in fragility curves. Two commonly used criteria for selecting the optimal EDP are identified in the literature [6,15,16] as efficiency and sufficiency/relative sufficiency.

In this study, the efficiency is related to the variability in the ductility μ for a given EDP value [17]. The $\beta_{d|EDP}$ (hereafter simply referred as β) is one of the quantitative measures used to assess the efficiency of the candidate EDPs. A lower value of β indicates less variability in the estimated value of μ . Another predictor used to assess efficiency is the regression R-squared (R^2) value, which indicates how well the regression model proposed in Eq. (2) fits the data. The value of R^2 ranges from zero to one, with values closer to one indicating a better fit of the model. In this study both β and R^2 were evaluated for all SDOF nonstructural components to compare the efficiency criterion for PFA and Sa. These two predictors are shown in Figure 2 for the regression models applied to the example case.

In regression analysis, sufficiency means that the selected independent variable such as the EDP is adequate to explain the variation in the dependent variable such as the ductility μ . Jalayer et al. [18] proposed relative a sufficiency approach to quantify the suitability of one EDP relative to another. This approach is denoted as $I(\mu|EDP_2|EDP_1)$, in which for this study EDP_2 and EDP_1 are Sa and PFA, respectively, and can be calculated as follows:

$$I(\mu|EDP_2|EDP_1) \cong \frac{1}{N} \sum_{i=1}^N \log_2 \left(\frac{\beta_{d|EDP_1} \phi \left(\frac{\ln(\mu_i) - \ln(a_2(edp_2)_i^{b_2})}{\beta_{d|EDP_2}} \right)}{\beta_{d|EDP_2} \phi \left(\frac{\ln(\mu_i) - \ln(a_1(edp_1)_i^{b_1})}{\beta_{d|EDP_1}} \right)} \right) \quad (4)$$

where ϕ is the standardized Gaussian probability distribution function. Relative sufficiency measure is expressed in units of bits of information, can be interpreted as the amount of information that is gained/lost on average about the uncertain response parameter μ by knowing EDP_2 instead of EDP_1 (relatively) [19]. A positive value of $I(\mu|EDP_2|EDP_1)$ implies that EDP_2 contains more information on μ than EDP_1 , which means that EDP_2 is more sufficient. Conversely, a negative value of $I(\mu|EDP_2|EDP_1)$ indicates that EDP_2 is less sufficient than EDP_1 in providing information.

In this study, the relative sufficiency approach was employed, and a sufficient EDP was defined as one whose estimations are not, or are less, affected by the floor on which the nonstructural component is mounted. For this purpose, because the SDOF nonstructural components with the same initial period installed on different floors were modeled using different strength f_y , the EDPs were normalized by f_y for the regression model to incorporate data from both the first floor and roof level.

RESULTS AND DISCUSSION

Figure 3 compares the β indicator from the regression models for all SDOF nonstructural components. Due to the floor motion frequency content filtering by the natural frequencies of the buildings, almost identical values for the β values are seen for regression models with PFA and Sa for the nonstructural components on the roof of the building. However, for the nonstructural components mounted on the first floor of the building, comparing the β values from regression models with two EDPs can be divided into three regions based on the range of the nonstructural components' periods: 0 to 0.2 s, 0.2 to 0.5 s, and 0.5 to 1 s. The β values for the SDOF nonstructural components having periods shorter than 0.2 s are similar but large for both regression models with PFA and Sa showing large variability in the estimated demands. For the SDOF nonstructural components with periods between 0.2 and 0.5 s, the β values are almost identical for regression models based on PFA and Sa, and those values remain around 0.4. For the SDOF nonstructural components having periods longer than 0.5 s, the regression models with Sa show lower β values than those with PFA, indicating Sa is the better EDP based on the β indicator. By increasing R , the β values for both regression models increase, and the difference between PFA and Sa also grows larger for components with a period of more than 0.5 s. This indicates that the regression model based on Sa is more optimal than PFA for the SDOF nonstructural components with lower strength. Furthermore, for periods longer than 0.4 s, the β values obtained from regression models with Sa are mostly lower than or equal to 0.4 across all ranges of the period and levels of strength. Mollaioli et al. [20] reported that β values ranging from 0.20 to 0.30 are generally indicative of good efficiency, while values between 0.30 and 0.40 are still considered reasonably acceptable.

Generally similar conclusions to those observed for the β values are also obtained for the R^2 values, as shown in Figure 4. However, unlike the β indicator, a larger R^2 value indicates a more efficient regression model. Also, in contrast to the β indicator, which showed that increasing R (reducing strength) decreases the efficiency of regression models with both Sa and PFA, increasing R increases R^2 values, indicating an increase in efficiency, for both Sa and PFA regression models. The reason is that unlike the β indicator which measures the standard deviation of residuals, R^2 is calculated as one minus the ratio of the sum

of squared residuals to the total sum of squares, which represents the distance of the data points from the mean. Although the squared residuals increase in the R^2 indicator like the β indicator, the denominator also increases due to the larger ductility experienced by the SDOF with a larger R , resulting in an increase in the distance of the data from the mean. Nonetheless, even when using the R^2 indicator, the regression model with S_a is shown to be more optimal than PFA for nonstructural components with periods longer than 0.5 s mounted on the first floor of the building.

To assess the EDPs' statistical independence with regard to the location of nonstructural components, the relative sufficiency of regression models for all SDOF nonstructural components is compared in Figure 5. Overall, for the SDOF nonstructural components with periods longer than 0.2 s and all strength levels, the calculated $I(\mu|S_a|PFA)$ is mostly positive, which indicates that the regression model with S_a is more sufficient than PFA. Also, for such SDOF nonstructural components, using S_a as the EDP provides mostly over 0.2 bits more information (on average) about the ductility per period, compared to using PFA. The results suggest that for the SDOF nonstructural components with periods shorter than 0.2 s, using PFA can provide conversely more information about ductility compared to S_a .

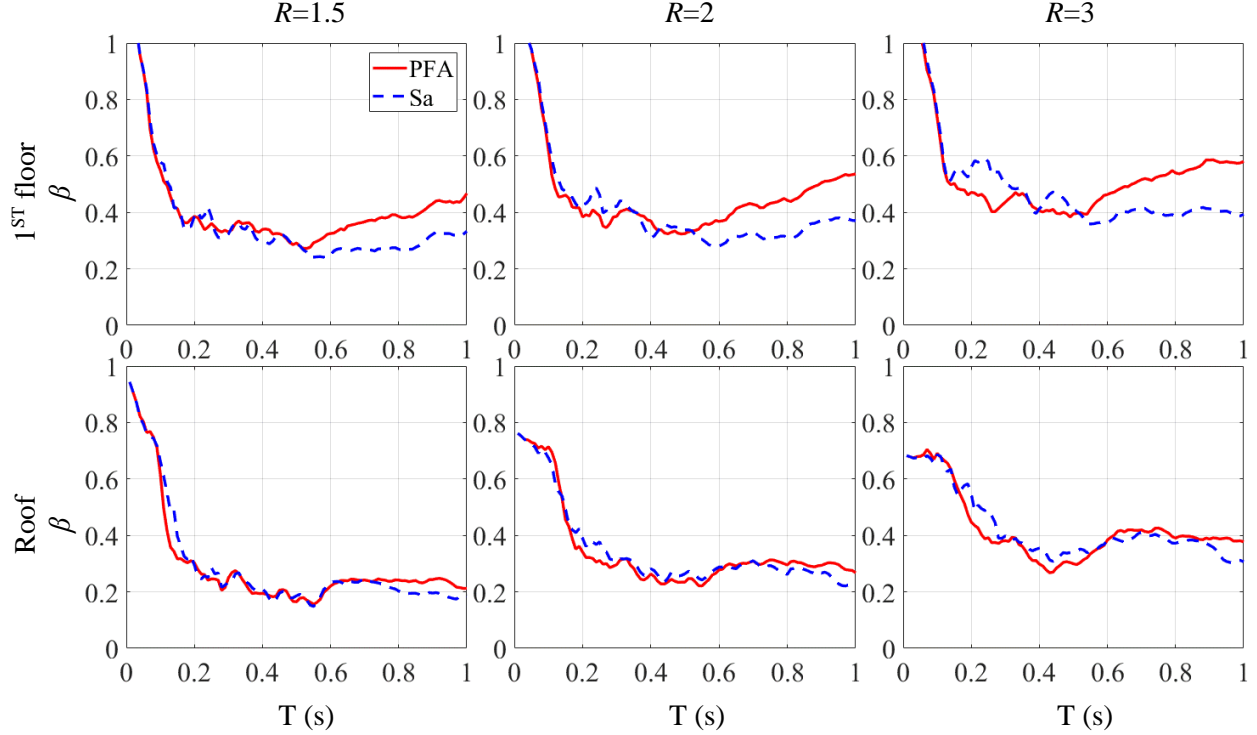


Figure 3: Comparing logarithmic standard deviations, β , of the regression models for all SDOF nonstructural components.

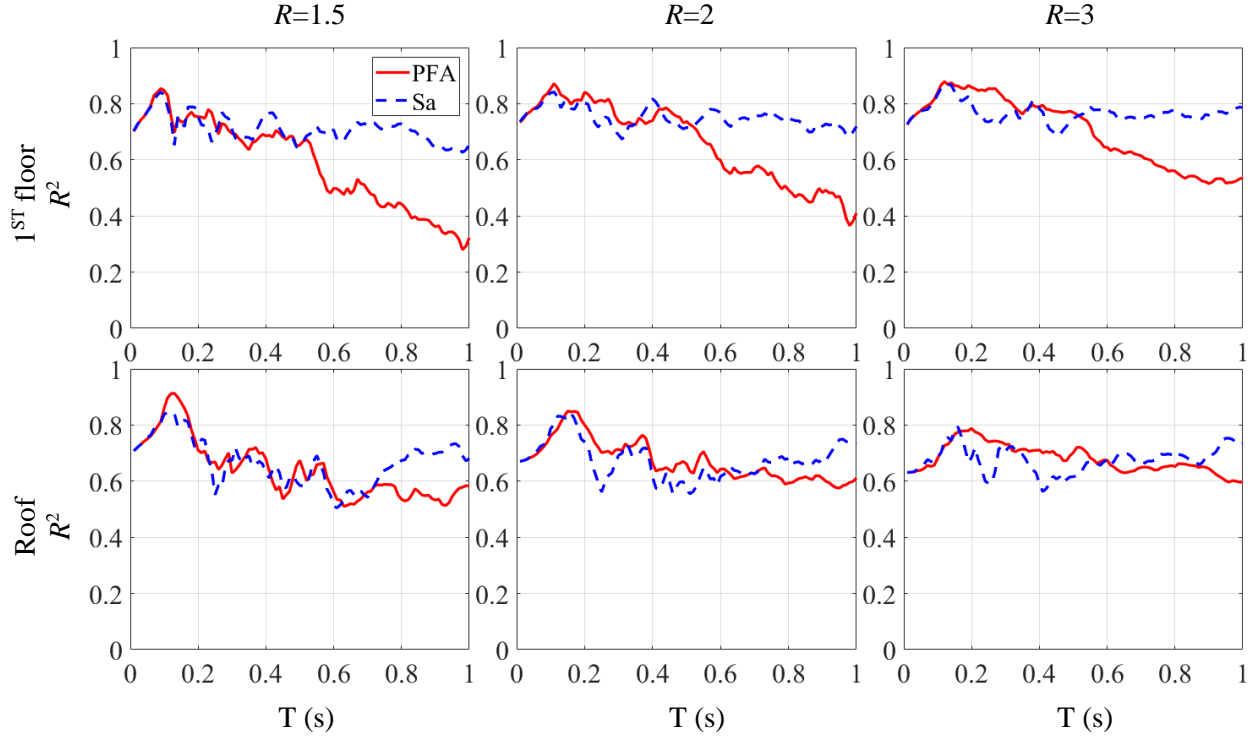


Figure 4: Comparing R^2 of the regression models for all SDOF nonstructural components.

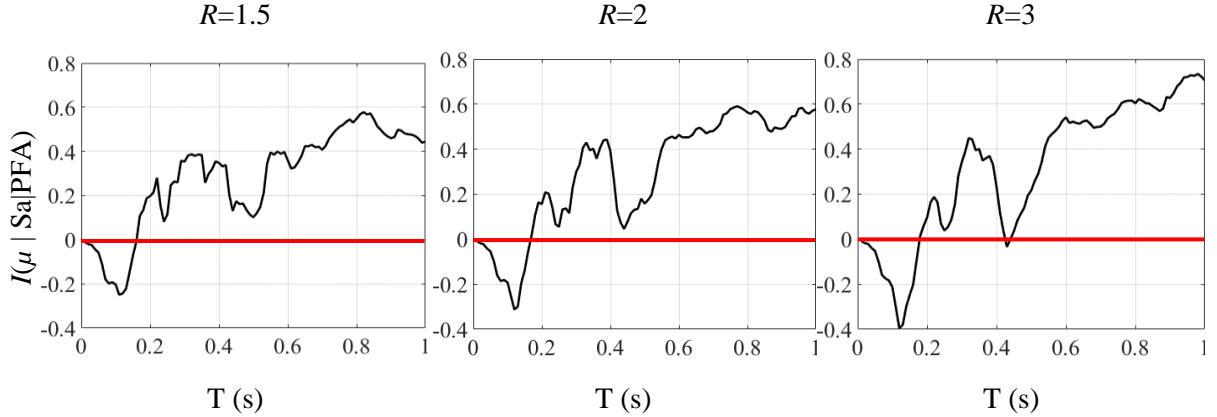


Figure 5: Comparing relative sufficiency, I , of the regression models for all SDOF nonstructural components to assess the level of EDPs' statistical independence with regard to the location of nonstructural components.

CONCLUSIONS

This study compared peak floor accelerations (PFAs) and fundamental period spectral accelerations (Sa) as engineering demand parameters (EDPs) for damage fragility curves of acceleration-sensitive nonstructural components. For this purpose, the behavior of nonstructural components was modeled using single-degree-of-freedom (SDOF) components with an elastic perfectly plastic material. Nonstructural components mounted on the first floor and roof of a building with six-story buckling-restrained braced frame were assessed based on floor motions from the first and roof levels that were obtained from nonlinear time-history analyses under the FEMA P695 [13] far-field ground motions set scaled to six intensity levels, ranging from 25% of the design earthquake (DE) to 2.0 times the maximum considered earthquake (MCE). Two lognormal regression models were developed using data pairs of ductility-PFA and ductility-Sa for each SDOF nonstructural component on each considered floor level. To assess the efficiency of candidate EDPs, the logarithmic standard deviation (β) and R-squared (R^2) were used as indicators and were calculated for each model. Also, to assess the statistical independence of the candidate EDPs based on the location of nonstructural components, the relative sufficiency between Sa and PFA was employed as an indicator. The main findings of this study are as follows:

- (1) For the nonstructural components installed on the roof of the building, the β values obtained from the regression models using PFA and S_a were similar over all ranges of component periods with all levels of strength, as the frequency content of the floor motions was filtered by the building's dynamic characteristics. However, for the nonstructural components installed on the first floor, the β values obtained from the regression models showed different trends depending on the period ranges of the nonstructural components. For components with periods shorter than 0.2 s, the β values are large for both regression models with PFA and S_a , indicating a large variability in the calculated ductility. For components with periods between 0.2 and 0.5 s, the β values are almost constant and identical for the models using PFA and S_a . For components with periods longer than 0.5 s, the regression models with S_a had lower β values than the models with PFA, indicating that S_a is the more efficient EDP for such nonstructural components installed in the lower levels of the building. Similar conclusions were also obtained using the R^2 indicator.
- (2) The results of the relative sufficiency analyses show that S_a is more sufficient than PFA for nonstructural components with periods longer than 0.2 s. However, for nonstructural components with periods shorter than 0.2 s, PFA is slightly more sufficient than S_a .

Based on the indicators used in this study, since S_a as an EDP demonstrated either better or at least equal sufficiency and efficiency when compared to PFA, it can be considered a better candidate EDP than PFA. However, further studies should be conducted, considering more advanced EDPs, in order to identify the best alternative candidate to PFA.

ACKNOWLEDGMENTS

This research was possible because of financial support from the Natural Sciences and Engineering Research Council of Canada (NSERC) and the Ontario Early Research Awards program.

REFERENCES

1. Carofilis W, Perrone D, O'Reilly GJ, Monteiro R, Filiatrault A. Seismic retrofit of existing school buildings in Italy: Performance evaluation and loss estimation. *Engineering Structures* 2020; **225**: 111243. DOI: <https://doi.org/10.1016/j.engstruct.2020.111243>.
2. Miranda E, Mosqueda G, Retamales R, Pekcan G. Performance of nonstructural components during the 27 February 2010 Chile earthquake. *Earthquake Spectra* 2012; **28**(S1): S453–S471. DOI: <https://doi.org/10.1193/1.4000032>.
3. FEMA P-58-3. *Seismic Performance Assessment of Buildings, Volume 3—Supporting Electronic Materials and Background Documentation: 3.1 Performance Assessment Calculation Tool (PACT)*. 3rd Edit. Version 3.1.2. Washington, DC, United States: prepared by the Applied Technology Council for the Federal Emergency Management Agency; 2018.
4. Housner GW and JPC. *Earthquake design criteria*. Berkeley, CA: Earthquake Engineering Research Institute; 1982.
5. Newmark NM, Hall WJ. Earthquake spectra and design. *Engineering Monographs on Earthquake Criteria* 1982.
6. Vargas-Alzate YF, Hurtado JE, Pujades LG. New insights into the relationship between seismic intensity measures and nonlinear structural response. *Bulletin of Earthquake Engineering* 2022; **20**(5): 2329–2365. DOI: <https://doi.org/10.1007/s10518-021-01283-x>.
7. Cornell CA, Jalayer F, Hamburger RO, Foutch DA. Probabilistic basis for 2000 SAC federal emergency management agency steel moment frame guidelines. *Journal of Structural Engineering* 2002; **128**(4): 526–533. DOI: [https://doi.org/10.1061/\(ASCE\)0733-9445\(2002\)128:4\(526\)](https://doi.org/10.1061/(ASCE)0733-9445(2002)128:4(526)).
8. Jalayer F, De Risi R, Manfredi G. Bayesian Cloud Analysis: Efficient structural fragility assessment using linear regression. *Bulletin of Earthquake Engineering* 2015; **13**(4): 1183–1203. DOI: <https://doi.org/10.1007/s10518-014-9692-z>.
9. Vargas-Alzate YF, Pujades LG, Barbat AH, Hurtado JE. An efficient methodology to estimate probabilistic seismic damage curves. *Journal of Structural Engineering* 2019; **145**(4): 04019010. DOI: [https://doi.org/10.1061/\(ASCE\)ST.1943-541X.0002290](https://doi.org/10.1061/(ASCE)ST.1943-541X.0002290).
10. ASCE/SEI 7-16. *Minimum design loads and associated criteria for buildings and other structures*. Reston, VA, United States: American Society of Civil Engineers; 2016.
11. Pacific Earthquake Engineering Research Centre (PEER). Open System for Earthquake Engineering Simulation v3.3.0 [Computer Software] 2021.
12. Zsarnóczy A. Experimental and numerical investigation of buckling restrained braced frames for eurocode conform

design procedure development. *Ph.D. Thesis*, Budapest, Hungary: Budapest University of Technology and Economics; 2013.

13. FEMA P695. *Quantification of Building Seismic Performance Factors*. Washington, DC, United States: prepared by the Applied Technology Council for the Federal Emergency Management Agency; 2009.
14. Nielson BG, DesRoches R. Seismic fragility methodology for highway bridges using a component level approach. *Earthquake Engineering and Structural Dynamics* 2007; **36**(6): 823–839. DOI: <https://doi.org/10.1002/eqe.655>.
15. Minas S, Galasso C. Accounting for spectral shape in simplified fragility analysis of case-study reinforced concrete frames. *Soil Dynamics and Earthquake Engineering* 2019; **119**: 91–103. DOI: <https://doi.org/10.1016/j.soildyn.2018.12.025>.
16. Ebrahimian H, Jalayer F, Lucchini A, Mollaioli F, Manfredi G. Preliminary ranking of alternative scalar and vector intensity measures of ground shaking. *Bulletin of Earthquake Engineering* 2015; **13**(10): 2805–2840. DOI: <https://doi.org/10.1007/s10518-015-9755-9>.
17. Padgett JE, Nielson BG, DesRoches R. Selection of optimal intensity measures in probabilistic seismic demand models of highway bridge portfolios. *Earthquake Engineering and Structural Dynamics* 2008; **37**(5): 711–725. DOI: <https://doi.org/10.1002/eqe.782>.
18. Jalayer F, Beck JL, Zareian F. Analyzing the sufficiency of alternative scalar and vector intensity measures of ground shaking based on information theory. *Journal of Engineering Mechanics* 2012; **138**(3): 307–316. DOI: [https://doi.org/10.1061/\(ASCE\)EM.1943-7889.0000327](https://doi.org/10.1061/(ASCE)EM.1943-7889.0000327).
19. Ebrahimian H, Jalayer F. Selection of seismic intensity measures for prescribed limit states using alternative nonlinear dynamic analysis methods. *Earthquake Engineering and Structural Dynamics* 2021; **50**(5): 1235–1250. DOI: [10.1002/eqe.3393](https://doi.org/10.1002/eqe.3393).
20. Mollaioli F, Lucchini A, Cheng Y, Monti G. Intensity measures for the seismic response prediction of base-isolated buildings. *Bulletin of Earthquake Engineering* 2013; **11**(5): 1841–1866. DOI: <https://doi.org/10.1007/s10518-013-9431-x>.